Optimization of Fluid Flow Distribution for a Skewed Flow Pattern in a Manifold

BURA SREENIVAS[1], JAN SKRINSKY[2]
[1]Department of Mechanical Engineering
Geethanjali College of Engineering and Technology
Cheeryal, Hyderabad, State of Telangana,
INDIA-501301
[2]Energy Research Centre,
VSB-TU Ostrava, 17. Listopadu 15, 70030,
CZECH REPUBLIC
burasreenivas@gmail.com, jan.skrinsky@vsb.cz

Abstract: Fluid flow optimization of an 8-parameter flow manifold for skewed flow distribution is dealt in this paper. We deal with a one-by-four manifold. We have to optimally locate the guide plates. The objective of the work is to minimize the standard deviation of the actual flow rates from the set points by controlling 8 parameters four of which are lengths and four of which are angles of deflection. The set points are flows in ratios of 40:30:20:10. We take the input as the 60 data points generated by the process of CFD. Using the combination of ordinary least squares and genetic algorithms we develop the minimization algorithm for the objective function. We have successfully evaluated the objective and 8 parameters for skewed flow distribution. Since we needed to achieve skewed distribution, the guide vanes were found to have greater role in offering resistances in flow apportionment as compared to the case of equal flow distribution, thus serving as high value resistors in the manifold circuit.

Keywords: Genetic algorithms, Least squares, Manifold, Skewed flow distribution

1 Introduction

The optimization algorithm employed in this work is from the category of non-gradient based algorithms which is the genetic algorithms. The use of genetic algorithms needs a fairly large population solution to start the optimization algorithm. The approach we need to follow is to use the meta models.

Elsayed & Lacor[1] and Elsayed & Lacor[2] built CFD simulations using the technique of ordinary least squares.

In order to facilitate principal component analysis(PCA) and support vector machine application, Li, Fevens & Krzyz[3] present an algorithm for clinical image segmentation. They classified the image processing process into two steps. These two steps are learning and segmentation.

Among many applications that are possible for PCA, Narasimhan[4] use PCA for model identification. They advocate a method for obtaining an approximate estimate of the model and error covariance matrix. They also provide an approach for model order determination and data scaling. The data scaling has been noted and used in this work. In addition to usual PCA, they have also evaluated results using iterative principal component analysis (IPCA). Shariati-rad and Hasani[5] employed PCA for determining the number of species that form during the equilibrium in the complex metal formation of ions with 1-10-phenantroline.

Coussement, Gicquel and Parente[6] employ PCA to investigate low dimensional manifold in the combustion process. They have also used a clustering method where they determine the number of principal components along with the number of clusters in MGLPCA.

Lindau et al.[7] constructed PCA to obtain statistical shape modelling for the virtual assemblies. Their paper demonstrates how PCA can be extended to larger applications to develop more tailor-made and robust applications that are suitable for the given domain. The application they considered were car-bodies.

Godoy, Vega, and Marchetti[8] present a detailed comparison between PCA and partial-least squares regression (PLSR) and brings out a relationship between them. They initially present the geometric properties of the decomposition of input(X-PCA) and output data(Y-PCA) in relation to the PCA. They have achieved the decomposition using partial

least squares regression. They have then presented the analogies of data subject to PLSR and YXPCA (input-output PCA). PLSR was found out to be more reliable for output-prediction, while YXPCA was more reliable for reducing redundancies. They have pointed out that the main difference between YXPCA and PLSR is that YXPCA does not distinguish between inputs and outputs and combines them in a single matrix, while PLSR differentiates between inputs and outputs. They have presented the derivations for the modeling for both PLSR and YXPCA in a separate sub-section. They have presented another section containing the relationship between PLSR and PCA.

Manifolds with guide vanes are employed in chemical process industries to achieve various kinds of flow distributions of various desirable ratios. The chemical process operations include heat exchangers; fuel cells etc. and their uses are versatile. The flow manifolds employed in this work use guide vanes to select flow distributions as against the rigid wall based manifolds that do not contain guide vanes. The advantage of placing guide vanes in the entrances of the outlets is that we can tune our desired flow distribution without the need to alter the construction of the walls of the manifolds. In our work we discuss the use of manifolds for skewed flow distribution.

Siddique et al.[12], discuss the design of efficient manifolds for microchannel heat exchanger for the purpose of efficient energy utilization. Wang and Wang[13] discuss a method for design of skewed flow distribution in manifolds.

A further work on flow optimization for skewed flow distribution was carried out by Srinivasan & Jayanti[9] . They used Box complex method for skewed flow apportionment, which is a gradient based method as an optimization algorithm while in this work we use evolutionary algorithms for optimization. From the literature, it is evident that CFD coupled with genetic algorithms is a versatile strategy but still has not been employed for skewed flow optimization. Till now only Box complex method has been employed for optimization of flow apportionment in a manifold. Thulasiram et al. [10] employed genetic algorithms for equal flow distribution for the first time. In this work, in the lines of Thulasiram et al. [10], we use genetic algorithm as the evolutionary algorithm and CFD as the evaluation mechanism.

Another difference with the work of Srinivasan & Jayanti[9] is that, in that work the evaluation of flow apportionment for first two cases is easier as it is not complex. But the 8 parameter problem which is the third case is fairly complex and results have further scope for improvement. Thus in this work we deal with the complex 8-parameter problem extensively which is the third case in the work of Srinivasan & Jayanti[9]. Besides Srinivasan & Jayanti[9], Avvari & Jayanti[11] had also carried a similar work. But the difference is that Avvari & Jayanti[11] employed normal gradient approach which is semi-analytical method, while Srinivasan & Jayanti[9] employed a fully computational method by using Box complex method. Thulasiram et al.[10], employed genetic algorithm and least square regression to optimize flow distribution in a manifold. But the type of flow distribution they employed is the equal flow distribution. This paper is a continuation of their work which was performed for a particular apportionment of flow which is the ratio of 25:25:25:25 in the four outlets. In this work also, we employ both genetic algorithm and least square regression, but the difference with their work is that we try to achieve skewed flow distribution which is an apportionment of 40:30:20:10 in the four outlets. Achieving this skewed distribution is more challenging than achieving equal flow distribution because based on the design of the manifold without guide vanes, there is a strong natural tendency to achieve flow distribution of equal apportionment. Thus, we have to alter the flow distribution forcefully by placing guide vanes. Therefore the functionality of the guide vanes becomes more pronounced in this work as compared to the work of Thulasiram et al. [10].

2 Problem Formulation

The objective of the present work is to explore the feasibility of utilizing genetic algorithms to the problem of determination of optimal flow distribution in a manifold by positioning the angles of the vanes and constructing the lengths of the vanes. To achieve this, the problem is formulated as a constrained optimization problem whose objective is to minimize the deviation of the actual flow rate from the set point in all the four outlets.

2.1 Description of geometry of the manifold

The geometric description of the 2-dimensional flow manifold is described in Fig.1. The fluid flow manifold consists of one inlet and four outlets where the breadth of the inlet duct is 0.1 m and that of the four outlet ducts is 0.05 m. The breadth header section is 0.1 m. The outlet ports are placed at a distance of 0.05 m with each other. Extended protruding sections of length 0.5 m at the inlet and 2 m at the outlets have been facilitated to achieve fully developed flow. Air at a velocity of 15 m/s is

specified at the inlet and 1 atmospheric pressure is specified at the outlets.

Physically it is not possible to exceed the length of the plates by 0.05 m and the angle of the guide vanes cannot be less than 90^0 as there is wall behind it (angles are measured in anti-clockwise direction). However as we see in the following sections more severe constraints are imposed on these parameters, which are more severe in the case of skewed flow distribution especially for skewed for distribution than those of equal flow distribution.

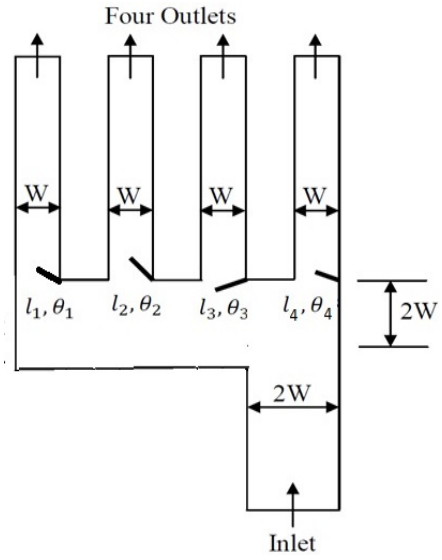

Fig. 1 Schematic of 8-parameter manifold

2.2 Formulation of the optimization problem

The aim of the current work is to accomplish a predetermined flow apportionment in the outlets. Hence the objective function is given as the additive square root of the deviations of the actual flow rates from the set points in the single channels. The two kinds of parameters which are length and angle of deflection of the guide vanes influence the flow in the manifold and hence the flow apportionment.

Hence the objective is obtained as the function of plate parameters. We try to optimize the deviation in the flow apportionment by changing the parameters which are length and angle of the guide vanes. Then, mathematically stating the optimization formulation becomes as:

Minimize f(x) where $f(x) = \sqrt{\sum_{j=1}^{q}(Q_j - \check{Q}_j)^2}$

and $x = \{\theta_i, l_i\}$ (1)

where, q is the total number of outlets, Q_j is the actual flow rate and $\check{Q}_j$ is the set point of flow rate through the j^{th} stream. x is the parametric set which consists of the angles of deflection θ_i and the lengths of the plates l_i for number of guide plates i.

Even though physical realizability limits are different we impose more severe constraints on the parameter values in equation (1) which are as:

$100° \leq \theta_1, \theta_2, \theta_3 \leq 260°$

$100° \leq \theta_4 \leq 160°$

$0.005 \leq l_1, l_2, l_3, l_4 \leq 0.045$

We always obtain non zero flow rates in any channel since the maximum length of the vanes is smaller than the duct breadth.

2.3 Multi-dimensional ordinary least squares regression using principal component analysis

Regression is the process of fitting a smooth function to a given set of independent data points. That data can be one-dimensional or multi-dimensional. In case the independent variable data is multidimensional then the regression of independent variables to the dependent variable is called multi-dimensional regression. In addition the data can be linear or nonlinear. If the data is nonlinear, then we call the method of regression employed as nonlinear regression.

PCA is a technique used to reduce the number of variables of data into fewer scores and instead of dealing with large number of variables we now deal with fewer numbers of scores. These scores are stored and subsequently used for further analysis. We can do data recovery or regression using these scores. In case of data recovery, however, based on the number of principal components employed, there is proportional loss in the data. In case of data storage, this is an advantage because sometimes as in case of image processing there is a need to store very large amounts of data and due to hardware restrictions we cannot store all the variables and so we need to store only scores.

The case of use of PCA in the case of flow manifold is to reduce redundancy and model the problem effectively. The reason why the modelling is effective is that there are few dominant variables among all the variables which affect the value of the objective function. When we are able to model the objective function as a function of these dominant variables, when can be able to do regression effectively because once accurate model is built, then we can do accurate regression. Since the modelling is based on use of principal components, this type of regression is termed Principal component regression (PCR).In our problem we have 8 independent variables and 1 dependent variable which is the objective function. However 8 parameters are redundant as there are few dominant variables which affect the objective function

strongly. The reason why PCA is particularly suitable to this 8 parameter problem is that this 8 parameter case has so many redundancies which reduce the effectiveness of the modelling phenomenon. PCA addressed such issues by reducing the redundancy. Hence PCR is ideally suited for this 8 parameter problem.

2.4 Evaluation of objective using least squares and optimization using genetic algorithms

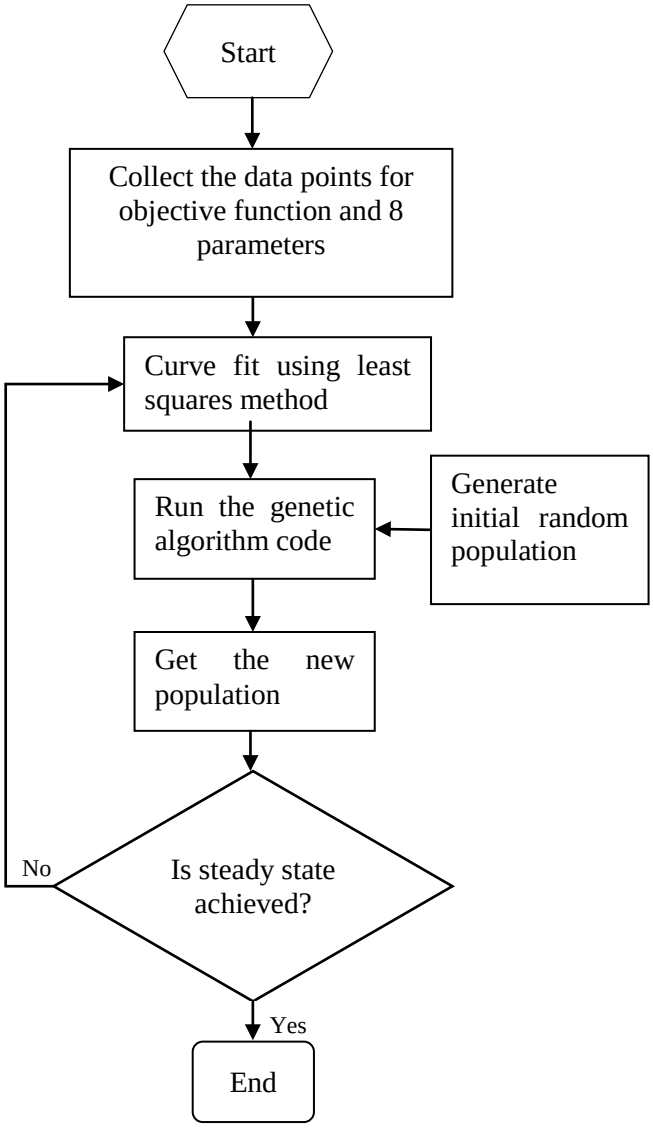

Fig. 2 Flow chart for the optimization code

60 data points are generated using CFD and we do multiple regressions to curve fit a model for the data. This model yields the objective function as a function of the 8 design parameters. Next initial random population is chosen in genetic algorithms. The values of the initial population are evaluated using the objective function that is curve-fitted by ordinary least squares. The optimum is evaluated and next again new population is chosen. This new population is again run through the genetic algorithms code and new objective is evaluated to generate another new population. In this way the code is run through many iterations till the steady state is achieved. The flow sheet is shown in Fig. 2.

Thulasiram et al.[10], used 50 data points for modelling. We carry out the work with a different set of points because the objective function is different even though the independent variables may be same. The reason is that we are dealing with skewed flow distribution where as Thulasiram et al.[10], employed equal flow distribution. The inlet flow is same in both the cases, which is 1.8375 kg/s of air. But the set points, which are the amounts of flow in the outlets is different in the two cases. Since the set point is different, so the deviation in the set point will also be different. In case of equal flow distribution employed by Thulasiram et al.[10], the set points at the outlets are 0.47 kg/sec of air in each of the four outlets. But since in our current work we are dealing with skewed flow distribution, the set points in the four outlets are 0.735 kg/sec, 0.55125 kg/sec, 0.3674 kg/sec and 0.18375 kg/sec.

3 Results and Discussions

60 random data points in 8-dimensions for the 8 parameter problem are generated and the value of the objective function is evaluated in ANSYS FLUENT work bench for the 60 data points. It is noted that each CFD evaluation is computationally expensive and the computational time increases as we try to make the grid finer. The point where we halt for grid refinement is discussed below.

3.1 Grid refinement and evaluation of objectives

The grid refinement is a very important topic in the CFD based evaluations. Unless the grid convergence is established for a sufficiently fine grid size, we cannot be sure that our results are accurate. The approach we take is that we check the results for a particular gird size, then we reduce the grid size by 25%-75%, check the values if they are same or not. If they are not same we further reduce the grid size. As we make the grid size finer and finer, at one point of sufficient finest grid we can expect the numerical solution to match the analytical solution after which however finer we go the solution is same. This point is selected for CFD based evaluations. In our case we have initially tried to simulate at 6mm and then do the same simulations for 3mm but the results are not same. Then we tried 3mm and 1.5 mm, still the results

varied. We try to evaluate grid convergence. It was found that grid converges at 1.5 mm. To demonstrate the grid convergence after 1.5 mm we choose two grids 1.5 mm and 1 mm values and show that the values obtained by CFD and the plots and graphs are same. This is illustrated in Fig.3, where we consider the pressure contours for same set of parameters, but for different grids. We observe similar pressure contours for both grid sized, thus confirming grid convergence.

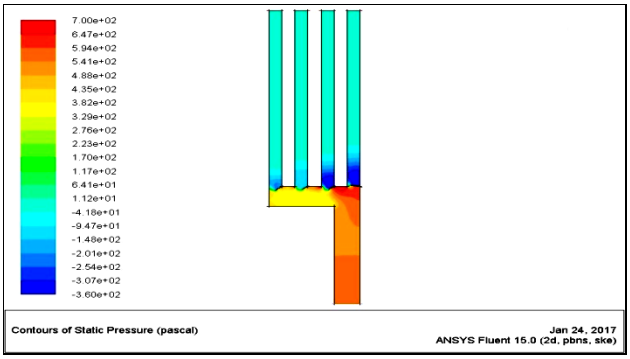

(a) 1.5 mm grid

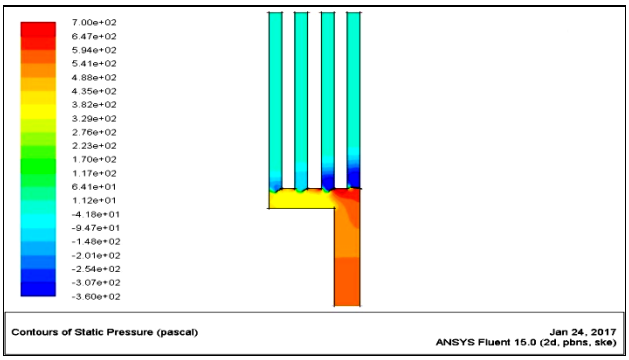

(b) 1 mm grid

Fig. 3 Grid convergence test for (a) 1.5 mm and (b) 1 mm grids

3.2 Use of genetic algorithms and ordinary least square regression

The angles are in range of 0° to 360°, while the lengths specified are in the range of 0 to 0.045m. Before employing genetic algorithms we scale and non-dimensionalize them to maintain uniformity in the code. We choose to non-dimensionalize the angles by 360^{o} and the lengths by 0.045 m which is the duct width of the manifold.

3.3 Validation of results using CFD simulations

Fig.4 shows the value of the standard deviation of the flow rates. It can be observed that observed that the standard deviation of the flow reaches a steady value after 110 iterations or generations. It attains a steady state value of $1.02 \times 10^{-3.2}$. Fig.5 shows the values of the design parameters for this case. As the case of Fig.4, the oscillations are arrested after 110 generations. The final values obtained by the 8 parameters are shown in Table 1. These are the values obtained before scaling that are shown in column 3 of Table 1. When we scale theta by 360^{0} and length by 0.045m, the values obtained are shown in column 4 of Table 1.

Table 1 Summary of values obtained

S. No.	Variable	Value obtained before dimensionalizing	Final values
1	θ_1	0.6944	250.121°
2	θ_2	0.5367	193.201°
3	θ_3	0.4700	169.2001°
4	θ_4	0.4860	174.986°
5	L_1	0.4333	0.0195 m
6	L_2	0.3622	0.0163 m
7	L_3	0.8511	0.0383 m
8	L_4	0.9822	0.0442 m
9	Standard Deviation (SD)	-	$1.02\times10^{-3.2}$
10	CFD based SD	-	0.0178

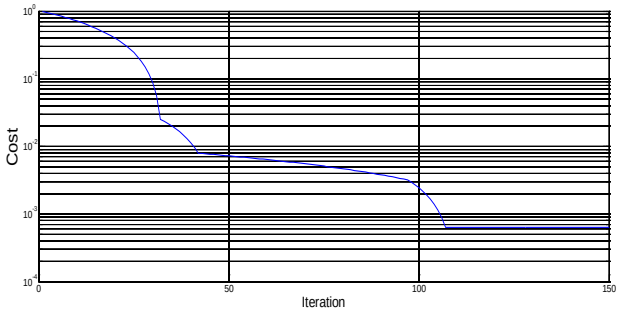

Fig. 4 Value of standard deviation before non-dimensionalizing

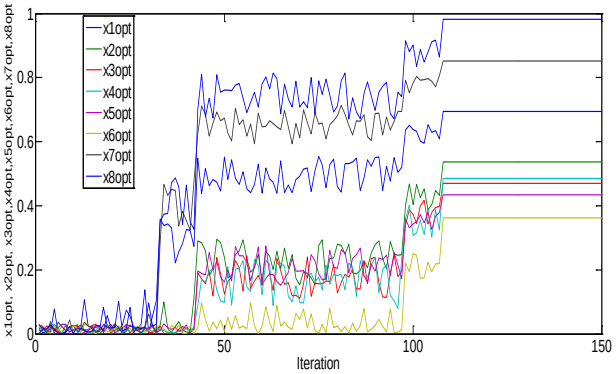

Fig. 5 Values of design parameters before non-dimensionalizing

Once the values of 8 parameters are obtained, we plug these values in CFD software and try to validate the results. We use ICEM software for

geometry creation and Fluent for running the simulations. When we successfully perform CFD simulations, we get the values of the mass fluxes at the four outlets. The value of fluxes obtained for these set of parameters are plugged in MATLAB to compute the value of the objective function.

The contours of static pressure for the final computed result of Table 1 are shown in Fig.6. It can be observed that there is uniform pressure distribution through all the legs of the manifold. We can observe that regions of low pressure are formed behind the vanes in the outlet leg of the manifolds. This is because low pressure eddies are generated at the back of the manifold. At the entrance of the inlet leg, the pressure is more than the pressure at the exit of the outlet legs. It can also be observed that the pressure at all the four outlet legs is same.

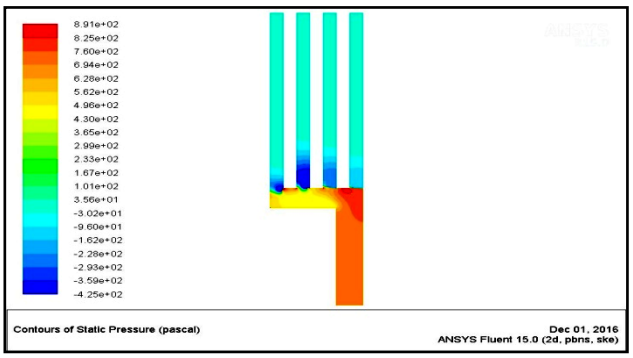

Fig. 6 Contours of static pressure for the final result

The contours of velocity by magnitude are shown in Fig.6. This is also observed to be uniform in all the four legs of the manifold. It can also be observed that the velocity is more at the inlet legs than the outlet legs. In addition it can be observed that the velocity behind the vanes is lowest while the velocity at the openings of the vanes is the highest. The velocity vectors are shown in Fig.8. These are arrows instead of colors. The magnitude of the velocity here is indicated by the length of the arrow. The arrows at the inlet are larger than the arrows at the outlet. It can be observed that the length of arrows show similar velocity magnitude in all the four legs in the manifold. The zoomed view of the velocity vectors corresponding to Fig.8 are shown for the header in Fig.9. It can be observed that the size of the arrows is larger in the opening of the outlet created by the vanes, while it is smaller behind the vanes. The Fig. 10-13 give further zoomed view of the velocity vectors in the four legs. Fig. 10 shows the velocity vectors for the first leg. As we can observe that for leg 1, the vane is situated at an angle of 250^{o} to the horizontal in anti-clockwise direction. With respect to the wall the angle is 160^{o}. Then length of the vane is 0.0195 m which is 40% of the leg width. We can observe that, near the vane, the flow direction is parallel to the vane. This is because the arrows in front of the vane are parallel to the vane and are pointed in the direction from the inlet to the outlet. However, we can see that this flow direction which is indicated by the direction of arrows is opposite behind the vanes. This indicates reverse flow behind the vanes. We can also observe that within the opening in the entrance of the outlet, as we move farther from the arrows, the flow is directed parallel to the walls. Some of the fluid hits the wall and rebounds back, which is also indicated by the direction and magnitude of the arrows.

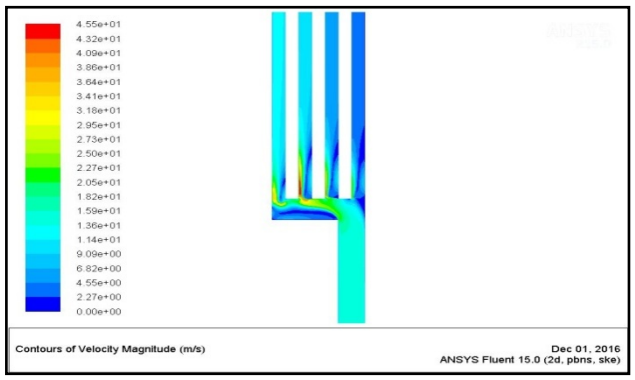

Fig. 7 Contours of velocity for the final result

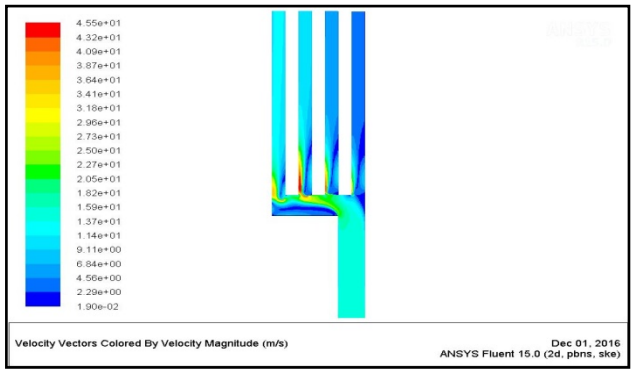

Fig. 8 Velocity vectors for the final result

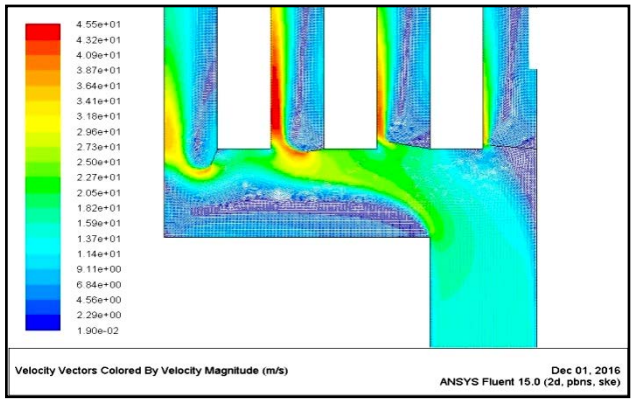

Fig. 9 Velocity vectors in the header

Fig. 11 shows the zoomed view of the velocity vectors for leg that is located second from the left side. We can observe that the vane is situated at an

angle of 193.201^{o} to the horizontal in anti-clockwise direction. In clockwise direction, the angle is 166.8^{o}. The length of the vane is 0.0163 m. Most of the fluid flowing from the header is going perpendicular to the vane due to inertia in the direction and hence a very little amount of fluid is flowing into the opening of the outlet leg. It can be also observed that the size of the arrows is larger in the left side than the right side. This happens due to the presence of the wall. It can also be observed that in the right side of the opening within the outlet leg, there is small amount of reverse flow.

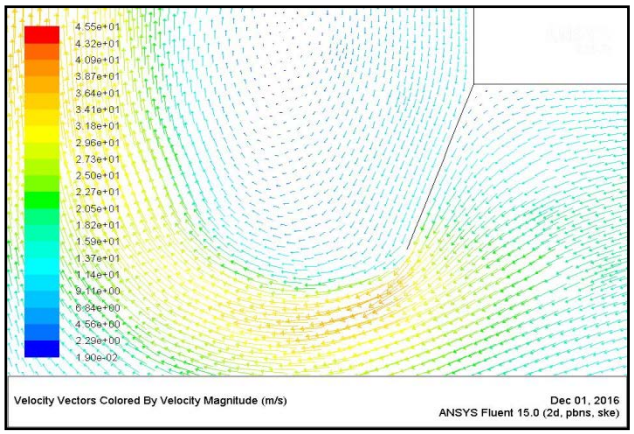

Fig.10 Velocity vectors (zoomed view) in leg 1(left most leg)

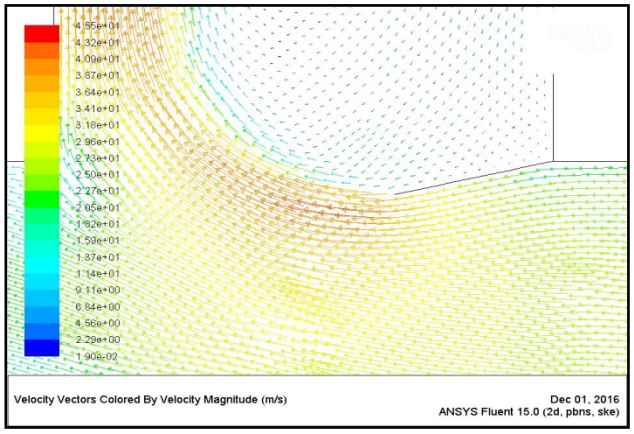

Fig.11 Velocity vectors (zoomed view) in leg 2

Fig.12 shows the zoomed view of the velocity vectors in the leg that is situated in third position from the left. The vane is situated at an angle of 169.2001^{o} in the anti-clockwise direction starting from the header wall. With respect to the outlet wall, the angle is 79.2001^{o}. The length of the vane is 0.0383 m which is about 80% of the vane opening. We can observe that because the vane is slanted in this case the flow is created in slanting direction and there is good amount of flow inside the opening due to the favorable position of the vanes. It can be also observed that towards the left side of the vane, there is strong magnitude of the flow, while behind the vane there is reverse flow. This illustrates the role of guide vane in the manifold application which is to appropriately control the flow orientation and magnitude.

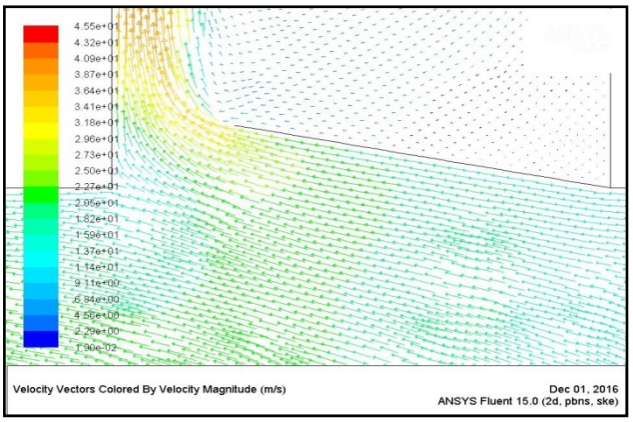

Fig.12 Velocity vectors (zoomed view) in leg 3

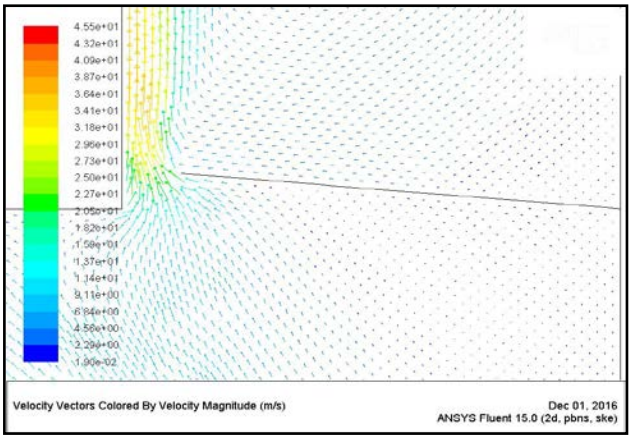

Fig.13 Velocity vectors (zoomed view) in leg 4 (right most leg)

Fig. 13 shows the zoomed view of the velocity vectors in the leg that is situated in fourth position from the left or first position from the right. The vane is situated at an angle of 174.986^{o} in the anti-clockwise direction starting from the header wall. With respect to the outlet wall, the angle is 84.986^{o}.The length of the vane is 0.0442 m which is nearly 90% of the vane opening. We can observe that because the vane is slanted in this case the flow is created in slanting direction and there is good amount of flow inside the opening due to the favourable position of the vanes. Since the outlet leg is situated directly in line with the flow inlet leg, we can observe that the flow is coming moving into the outleg leg. The role of guide vane becomes more predominant for this first vane than the other 3 vanes of the other legs. This is because more flow deflection is needed in this leg. It can be observed that in the vicinity of the vane, the flow magnitude is less, as it is rightly indicated by the length of the arrows. There is even small amount of reverse flow,

especially behind the vanes and in front of the vanes. But still the flow in the opening to the left of the vane is very large due to inertia of direction from the inlet.

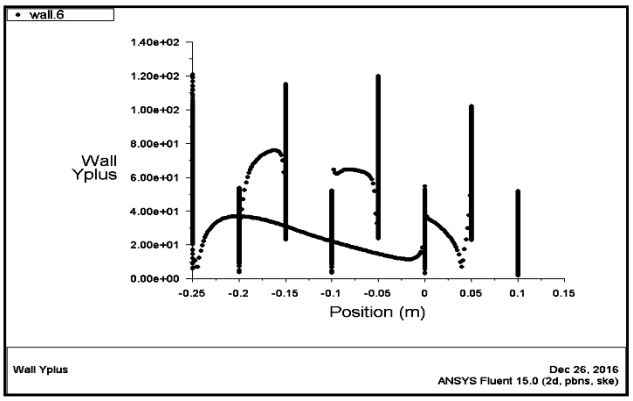

Fig. 14 Wall Y plus values for the final result

Fig. 14 shows the wall Y plus values of the obtained results. The expected value of wall Y plus for a reasonably good CFD computation is around 30. We find that most of the times the wall Y Plus value is 30, thus confirming the success of our CFD simulations

4 Conclusions

In this paper, we achieved flow apportionment for skewed flow distribution in a manifold. We used genetic algorithm and modelling through ordinary least squares to solve for flow minimization in a manifold problem. It has been found that a significant improvement in the standard deviation has been obtained with very less CFD computations. If we observe the standard deviations of the initially chosen 60 random data points, the lowest value is 0.0489. But using method of this work, we have achieved a standard deviation of 0.0178. Therefore the optimization using genetic algorithms combined with least squares regression has yielded an improvised solution. Further it is noted that we have achieved this result without resorting to computationally expensive CFD simulations. The velocity contours obtained for the final solution through CFD simulations have been demonstrated for illustration.

References:

[1] K. Elsayed and C. Lacor, "Modeling, analysis and optimization of aircyclones using artificial neural network, response surface methodology and CFD simulation approaches," *Powder Technology*, vol. 212, no. 1, pp. 115–133, 2011.

[2] K. Elsayed and C. Lacor, "CFD modeling and multi-objective optimization of cyclone geometry using desirability function, Artificial neural networks and genetic algorithms," *Applied Mathematical Modelling*, 2013.

[3] S. Li, T. Fevens, and A. Krzyz, "Automatic clinical image segmentation using pathological modeling , PCA and SVM," vol. 19, pp. 403–410, 2006.

[4] S. L. S. Narasimhan, "Model identification and error covariance matrix estimation from noisy data using PCA," vol. 16, pp. 146–155, 2008.

[5] M. Shariati-rad and M. Hasani, "Analytica Chimica Acta Principle component analysis (PCA) and second-order global hard-modelling for the complete resolution of transition metal ions complex formation with," vol. 648, pp. 60–70, 2009.

[6] A. Coussement, O. Gicquel, and A. Parente, "MG-local-PCA method for reduced order combustion modeling," *Proceedings of the Combustion Institute*, vol. 34, no. 1, pp. 1117–1123, 2013.

[7] B. Lindau, L. Lindkvist, A. Andersson, and R. Söderberg, "Statistical shape modeling in virtual assembly using PCA-technique," *Journal of Manufacturing Systems*, vol. 32, no. 3, pp. 456–463, 2013.

[8] J. L. Godoy, J. R. Vega, and J. L. Marchetti, "Chemometrics and Intelligent Laboratory Systems Relationships between PCA and PLS-regression," *Chemometrics and Intelligent Laboratory Systems*, vol. 130, pp. 182–191, 2014.

[9] K. Srinivasan and S. Jayanti, "An automated procedure for the optimal positioning of guide plates in a flow manifold using Box complex method," *Applied Thermal Engineering*, vol. 76, pp. 292–300, 2015.

[10] A. R. Thulasiram, B. Sreenivas, and S. Jayanti, "Flow Apportionment in a Manifold by using Genetic Algorithm and Least Squares Regression," vol. 11, 2017.

[11] R. Avvari and S. Jayanti, "Flow apportionment algorithm for optimization of power plant ducting," *Applied Thermal Engineering*, vol. 94, pp. 715–726, 2016.

[12] O. K. Siddiqui and S. M. Zubair, "E ffi cient energy utilization through proper design of microchannel heat exchanger manifolds : A comprehensive review," *Renewable and Sustainable Energy Reviews*, vol. 74, no. December 2016, pp. 969–1002, 2017.

[13] J. Wang and H. Wang, "Discrete method for design of flow distribution in manifolds," *Applied Thermal Engineering*, vol. 89, pp. 927–945, 2015.